A Role for the Human Nucleotide-binding Domain, Leucine-rich Repeat-containing Family Member NLRC5 in Antiviral Responses* §

Received for publication, February 3, 2010, and in revised form, June 5, 2010 Published, JBC Papers in Press, June 10, 2010, DOI 10.1074/jbc.M110.109736

Andreas Neerincx † , Katja Lautz † , Maureen Menning † , Elisabeth Kremmer $^{\circ}$, Paola Zigrino ¶ , Marianna Hösel $^{\parallel **}$, Hildegard Büning **, Robert Schwarzenbacher*, and Thomas A. Kufer*

From the † Institute for Medical Microbiology, Immunology and Hygiene, University of Cologne, 50931 Cologne, Germany, $^{\$}$ Institute of Molecular Immunology, Helmholtz Zentrum München, 81377 München, Germany, [¶]Department of Dermatology, University of Cologne, 50937 Cologne, Germany, ^{||}Klinik I für Innere Medizin, University of Cologne, 50937 Cologne, Germany, **Zentrum für Molekulare Medizin Köln, University of Cologne, 50931 Cologne, Germany, and ^{‡‡}Department of Molecular Biology, University of Salzburg, 5020 Salzburg, Austria

Proteins of the nucleotide-binding domain, leucine-rich repeat (NLR)-containing family recently gained attention as important components of the innate immune system. Although over 20 of these proteins are present in humans, only a few members including the cytosolic pattern recognition receptors NOD1, NOD2, and NLRP3 have been analyzed extensively. These NLRs were shown to be pivotal for mounting innate immune response toward microbial invasion. Here we report on the characterization of human NLRC5 and provide evidence that this NLR has a function in innate immune responses. We found that NLRC5 is a cytosolic protein expressed predominantly in hematopoetic cells. NLRC5 mRNA and protein expression was inducible by the double-stranded RNA analog poly(I·C) and Sendai virus. Overexpression of NLRC5 failed to trigger inflammatory responses such as the NF-κB or interferon pathways in HEK293T cells. However, knockdown of endogenous NLRC5 reduced Sendai virus- and poly(I·C)-mediated type I interferon pathway-dependent responses in THP-1 cells and human primary dermal fibroblasts. Taken together, this defines a function for NLRC5 in anti-viral innate immune responses.

Innate immunity and induction of adaptive immune responses are based on the recognition of conserved signatures of microbes and "danger signals" released from infected host cells. These pathogen-associated molecular patterns (PAMPs)² and danger-associated molecular patterns (DAMPs) are recognized by so-called pattern recognition receptors in the host and trigger inflammatory responses (1). Different types of pattern recognition receptors show distinct subcellular localization, allowing the host to react to extracellular, vesicular, and cytosolic presented PAMPs and DAMPs. One class of pattern recognition receptors, the nucleotide-binding domain, leucine-rich repeat (NLR)-containing protein family, gained much attention because it was shown that members of this family are critically involved in mounting immune responses to bacterial peptidoglycan fragments and in controlling release of the key inflammatory cytokine interleukin- 1β (2–4). Over 20 NLRs are encoded in the human genome. As a hallmark they share a tripartite molecular architecture with a centrally located ATPase domain, a NACHT domain (domain present in NAIP, CIITA, HET-E, TP-1) that mediates oligomerization and activation of these proteins, followed by a leucine-rich repeat region (LRR) at the C terminus. With the only exceptions of NLRX1 and NAIP, the N-terminal part of the NLRs consists of a domain that adopts a death domain fold. Most NLR members thereby have either a caspase activation and recruitment domain (CARD) or a pyrin domain (PYD), connecting the respective NLR to different downstream signaling events (2). Well studied examples of CARD domain-containing NLRs are NOD1 and NOD2, which react to peptidoglycan fragments and lead to NF- κ B, MAPK, and caspase activation (3). Examples of PYD containing NLRs comprise NLRP1 and NLRP3, which form high molecular weight platforms, so-called inflammasomes that lead to activation of caspase-1 and subsequent interleukin- 1β release upon encounter of DAMPs and certain PAMPs (4).

NLRC5 (alternatively named NOD27 or CLR16.1) is an interesting exception in the NLR family. It has a typical NLR architecture but contains an effector domain, predicted to adopt a death domain (DD) fold without obvious homology to the CARD and PYD domains found in other NLRs. Furthermore, it possesses the longest LRR domain of all human NLR members. Alignment of the LRR domains shows that within the NLR family NLRC5 is most closely related to

dehydrogenase; IFN, interferon; siRNA, small interfering RNA; GFP, green fluorescent protein; HRP, horseradish peroxidase; ELISA, enzyme-linked immunosorbent assay; RANTES, regulated upon activation, normal T cell expressed, and secreted.



^{*} This work was supported by Deutsche Forschungsgemeinschaft Grants SFB670-N01 (to T. A. K.) and SFB670-TP8 (to M. H. and H. B.) and European Commission Grant MEXT-CT-2006-033534 (to R. S. and A. N.).

The on-line version of this article (available at http://www.jbc.org) contains supplemental Figs. S1-S3.

¹ To whom correspondence should be addressed: Joseph-Stelzmann-Str. 9, Geb. 37, 50931 Cologne, Germany. Tel.: 49-221-478-7279; Fax: 49-221-478-7288; E-mail: thomas.kufer@uk-koeln.de.

² The abbreviations used are: PAMP, pathogen-associated molecular pattern; DAMP, danger-associated molecular pattern; LRR, leucine-rich repeats; CARD, caspase activation and recruitment domain; PYD, pyrin domain; DD, death domain; SeV, Sendai virus; NLR, nucleotide-binding domain, leucine-rich repeat-containing; MAPK, mitogen-activated protein kinase; RT, reverse transcription; GAPDH, glyceraldehyde-3-phosphate

NOD1, NOD2, and NLRC3 (5). This is further confirmed by sequence comparison of the NACHT domains, which puts NLRC5 in evolutionary vicinity to NOD1, NOD2, and NLRC3 (6,7). NOD1 and NOD2 are well characterized NLRs with a critical function in controlling immune responses toward bacterial challenge and likely also viral challenge (2, 8). Moreover, NLRC3 was proposed to function as a negative regulator in T cells (9). This suggested that NLRC5 might also be involved in innate immune responses in humans. Interestingly, all of the mentioned NLRs are localized on the same chromosomal region. However, the biological relevance of this fact remains elusive (10). In the present study we characterize human NLRC5, revealing a function in antiviral innate immune responses in human cells.

EXPERIMENTAL PROCEDURES

Cells and Cell Culture-Primary human dermal fibroblasts were obtained by outgrowth from skin explants as previously described (11). The cells were cultured in Dulbecco's modified Eagle's medium (Biochrom AG) supplemented with 10% heatinactivated fetal calf serum (BioWest), 2 mm glutamine, and 100 units/ml each of penicillin and streptomycin (Biochrom AG) in 5% CO₂ at 37 °C in a humidified atmosphere. The fibroblasts were passaged by trypsinization at a ratio of 1:2 every 3 days and used at passages 1-4. HEK293T, HeLa, and CaCo2 cells were grown at 37 °C with 5% CO2 in Dulbecco's modified Eagle's medium containing 10% heat-inactivated fetal calf serum and penicillin-streptomycin. THP-1 cells were maintained in VLE RPMI 1640 (Biochrom AG) containing 10% heat-inactivated fetal calf serum, penicillin-streptomycin, and 100 µg/ml Zeocin (Invivogen) in the case of THP-1 blue. The cells were continuously tested for mycoplasma contamination by PCR. Poly(I·C), lipopolysaccharides (ultrapure lipopolysaccharide, Escherichia coli 0111:B4), muramyl di-peptide, and phorbol 12-myristate 13-acetate were obtained from Invivogen (France).

Sendai virus (hen egg allantoid fluid) was obtained from Charles River Laboratories. For stimulation 133 hemagglutination units (HAU)/ml were used for HEK293T cells, 160 HAU/ml for HeLa cells and primary fibroblasts, and 80 HAU/ml for THP-1 cells.

Plasmids and Reagents—Human NLRC5 (NP_115582) was obtained by nested PCR from a human leukocyte cDNA library (Marathon-ready cDNA; Clontech) using the following primers: fwd1, CGTGGGGACCCTAGAGCACCTATCA; rev1, GCATCACTTGGCTGGATTCCAAAGG; fwd2, CTGC-AGGAATTCGATATCATGGACCCCGTTGGCCTCCAG; and rev2, CGGGCCCCCCCTCGAGTCAAGTACCCCAAGGG-GCCTG. The PCR products were cloned by EcoRV-XhoI into pCMV-Tag2B. The FLAG-NOD1 plasmid is described in Ref. 12, and FLAG-NLRP3 was a kind gift from Fabio Martinon. All of the plasmids were verified by DNA sequencing.

Generation of Monoclonal Antibodies against NLRC5—Two peptides of NLRC5 (117 HHGLKRPHQSCGSSPRRKQC 136) and (1855 FFDNQPQAPWGT 1866) were synthesized and coupled to bovine serum albumin or ovalbumin (PSL, Heidelberg, Germany). The rats were immunized with 50 $\mu \rm g$ of peptide-ovalbumin using CpG 2006 and incomplete Freund adjuvant as adjuvants. Anti-NLRC5 3H8 (epitope amino acids 1855–1866) of

the rat immunoglobulin G2a (IgG2a) subclass was used in this study

RT-PCR and Quantitative PCR—End point RT-PCR was performed using Taq polymerase (Fermentas) on cDNA obtained from isolated RNA of the indicated cell lines. RNA was isolated using the RNeasy kit (Qiagen), and 1 µg of total RNA was transcribed into cDNA using a First Strand cDNA synthesis kit with an oligo(dT) primer (Fermentas). The following primer pairs were used: NLRC5fw, CTCCTCACCTCCAGCTTCAC; NLRC5rev, GTTATTCCAGAGGCGGATGA; NLRC5iso3fw, AGGCTGTGGGCAGATAGAGA; NLRC5iso3rev, ACCAG-GCATCCCCAGC; NLRC5iso4fw, TTTGCACTTCAGATCC-AACG; NLRC5iso4rev, GATCAAGCAAACCGGAGATG; GAPDHfw, GGTATCGTGGAAGGACTCATGAC; and GAP-DHrev, ATGCCAGTGAGCTTCCCGTTCAG. The RANTES primers were published in Ref. 13. The PCR products were separated by agarose gel electrophoresis and visualized using ethidium bromide.

For gene expression profiling cDNA from human tissues MTC multiple tissue cDNA panels (Clontech) were used. Quantitative PCRs for measuring NLRC5 expression were performed on an IQ-5 cycler (Bio-Rad) using SYBR-green Master mix (Bio-Rad) with the primer pairs indicated above. The data from triplicate measurements were analyzed using the $\Delta \Delta D T$ method, normalized to glyceraldehyde-3-phosphate dehydrogenase (GAPDH) gene expression (Bio-Rad IQ5 software package). The results were verified by end point PCR using an independent primer pair specific for NLRC5.

IFN- β and IP-10 mRNA real time PCRs were performed with the LightCyclerTM system using the LC FastStart DNA MasterPLUS SYBR Green 1 Kit (Roche Applied Science) and sequence-specific oligonucleotide primer pairs: IFNbfw, 5′-GCCGCATTGACCATCT-3′; IFNbrev, 5′-GCACAGTGAC-TGTACTCC-3′; IP-10fwd, 5′-ACTGTACGCTGTACCT-3′; IP-10rev, 5′-TGGCCTTCGATTCTGGA-3′; GAPDHfw, 5′-GGTATCGTGGAAGGACT-3′; and GAPDHrev, 5′-GGGTG-TCGCTGTTGAA-3′. For relative quantification, the cDNA levels were determined relative to GAPDH gene expression and normalized to a dilution series of calibrator cDNA using the Relative Quantification Software (Roche Applied Science) as described (14).

siRNA Knockdown—Gene silencing was performed by transfection of siRNA duplexes (Qiagen) using HiPerfect (Qiagen). THP-1 cells were differentiated with 100 nm phorbol 12-myristate 13-acetate 16 h prior siRNA transfection. 72 h after siRNA treatment, the cells were stimulated as indicated. After additional 16 h, the supernatant and cells were collected. RNA was prepared by combining triplicates using the RNeasy kit (Qiagen) according to the manufacturer's instructions. For gene expression analysis, 1 µg of total RNA was transcribed into cDNA using a First Strand cDNA synthesis kit with an oligo(dT) primer (Fermentas). HeLa cells were transfected with 10 nm siRNA using Hiperfect (Qiagen) transfection reagent according to the manufacturer's conditions and stimulated 48 h after siRNA transfection. The following siRNAs were used: NLRC5-1, CAGGGTTCTCTCCCTGTTAGA; NLRC5-4, CTGCTGATCTTTGATGGGCTA; and AllStars negative control (Qiagen). siRNAs for TBK1- and TLR3-specific siRNA



duplexes were synthesized from Qiagen as described in Refs. 15 and 16.

Luciferase Assays—Activation of inflammatory pathways was measured using a modification of the luciferase reporter assay described previously (17). The indicated luciferase-reporter plasmid (PathDetect system; Agilent Stratagene) and FLAG-NLRC5 expression plasmid along with a plasmid expressing β -galactosidase were transfected. The cells were stimulated immediately after transfection as indicated. After 16 h of incubation, the cells were lysed, and the luciferase activity was measured. Luciferase activity was normalized to β -galactosidase activity. The means and standard deviations were calculated from triplets and are representative of at least three independent experiments.

Indirect Immunofluorescence—The cells were fixed in 3% paraformaldehyde in phosphate-buffered saline and permeabilized with 0.5% Triton X-100 for 5 min. The cells were incubated in 3% bovine serum albumin in phosphate-buffered saline. The primary antibody was mouse anti-FLAG M2 (F3165; Sigma-Aldrich). The secondary antibody was Alexa 488-conjugated goat anti-mouse IgG (Molecular Probes). DNA was stained with 4',6-diamidino-2-phenylindole, dihydrochloride (Molecular Probes). The images were acquired on an Olympus FV-1000 confocal microscope and processed using ImageJ.

Immunoblotting and Immunoprecipitations—Immunoprecipitations were conducted as described previously (17). The proteins were detected after SDS-PAGE and blotting to a nitrocellulose membrane by subsequent incubation with primary and secondary antibodies and by a final incubation with Super-Signal West Femto maximum sensitivity substrate (Pierce). The signals were recorded using a Fujifilm LAS4000 ECL camera system.

Primary antibodies were mouse anti-FLAG M2 (Sigma-Aldrich; antibody F3165), mouse anti-GFP (Roche Applied Science; antibody 11814460001), mouse anti-α-tubulin (Sigma; antibody T7816), rabbit anti-TBK1 (Santa Cruz; antibody sc-52957), rabbit anti-GAPDH (Santa Cruz; antibody sc-25778), or rat anti-NLRC5 (this study; antibody 3H8). The secondary antibodies were HRP-conjugated goat anti-mouse IgG (Bio-Rad; antibody 170-6616), HRP-conjugated goat anti-rabbit IgG (Bio-Rad; antibody 170-6515), HRP-conjugated goat anti-rat IgG (Jackson; antibody 112-035-068), and HRP-conjugated rabbit antigoat IgG (Bio-Rad; antibody 172-1034).

Detection of Cytokines—For detection of type I interferons, the secreted alkaline phosphatase reporter HEK-BlueTM IFN- α/β cells (Invivogen) were seeded in 96-well plates and incubated with the appropriately diluted supernatant for 16 h. Secreted alkaline phosphatase activity was determined with QUANTI-BlueTM (Invivogen) according to the manufacturer's protocol. Selectivity and specificity of the assay was determined using recombinant IFN- α and IFN- γ . The measurements were performed in triplicate. The data are representative of at least three independent experiments.

For cytokine profiling, human cytokine array kit (R & D Systems) was used. Quantification was performed by recording the signal on a LAS4000 ECL camera system and densitometric quantification to the internal controls after background subtraction (ImageJ). ELISA for IFN-β, RANTES, and IP-10 was performed using a MultiAnalyte ELISArray kit (MEH-007A; SABiosciences) according to the manufacturer's instructions.

RANTES was measured using a human CCL5 ELISA kit (DY278; R & D Systems) according to the manufacturer's conditions. The measurements were conducted from at least two biological replicates in at least two appropriate dilutions.

Statistics—The data were analyzed using two-sided Student's t test. The differences were regarded as significant (*) when p <0.05 and highly significant (**) when p < 0.005.

RESULTS

NLRC5 Structure and Expression—Sequence comparisons of NLRC5 show the same overall multidomain architecture composed of effector, NACHT, winged helix, superhelical, and LRR domains, found in all other human NLRs. Differences exist in the type of effector domain and the significantly longer LRR receptor domain. The NLRC5 effector domain (residues 1–101) is composed of five α -helices and shows no sequence homology to CARD or PYD domains. This indicates that the NLRC5 effector domain is structurally similar to CARD and PYD domains but features a different interface. The NACHT domain shows all typical features important for nucleotide hydrolysis followed by a winged helix domain and a superhelical domain. Thus, NLRC5 is a typical Apaf-like ATPase likely capable of ATP hydrolysis required for conformational changes that lead to activation. The LRR domain in NLRC5 differs from other LRRs in NLRs in respect to its length of more than 1000 residues. Structurally, leucine-rich repeats of that length should form more than a full LRR circle, resulting in a LRR helix (Fig. 1A).

To decipher the basal expression pattern of NLRC5 mRNA quantitative PCR and end point PCR were performed with cDNA obtained from different tissue and cell lines, respectively. NLRC5 was predominantly expressed in select tissues including immune cells and organs. In line with available microarray data (BioGPS), the highest expression of NLRC5 was observed in cells of the hematopoietic compartment (Fig. 1B). NLRC5 was expressed the highest in T cells (CD4⁺ and CD8⁺) and B cells (CD19⁺) and to a lesser extent in macrophages (CD14⁺) and tissues such as lymph nodes, spleen, bone marrow, and tonsils (Fig. 1B). Accordingly, we found high expression of NLRC5 mRNA in cell lines of thymoid (Jurkat) and myeloid (THP-1) origin, whereas epithelial cell lines derived from human embryonic kidney (HEK293T) and colon (CaCo2) only showed marginal expression of NLRC5 (Fig. 1C). However, robust basal NLRC5 expression was observed in the cervix carcinoma cell line HeLa (Fig. 1C).

Next, we cloned the NLRC5 open reading frame from a human leukocyte cDNA library. During the cloning procedure, different splice variants were obtained. Five of these have been reported in databases. All shared a conserved 5' region encoding the DD and the NACHT domain but differed in the length of the LRRs (Fig. 1D). Modeling of the NLRC5 structure indicated that the unusually long LRR domain of NLRC5 might form a large helical conformation (Fig. 1A). Thus, the cloned isoforms with truncated LRRs might give rise not only to different elicitor sensing specific-



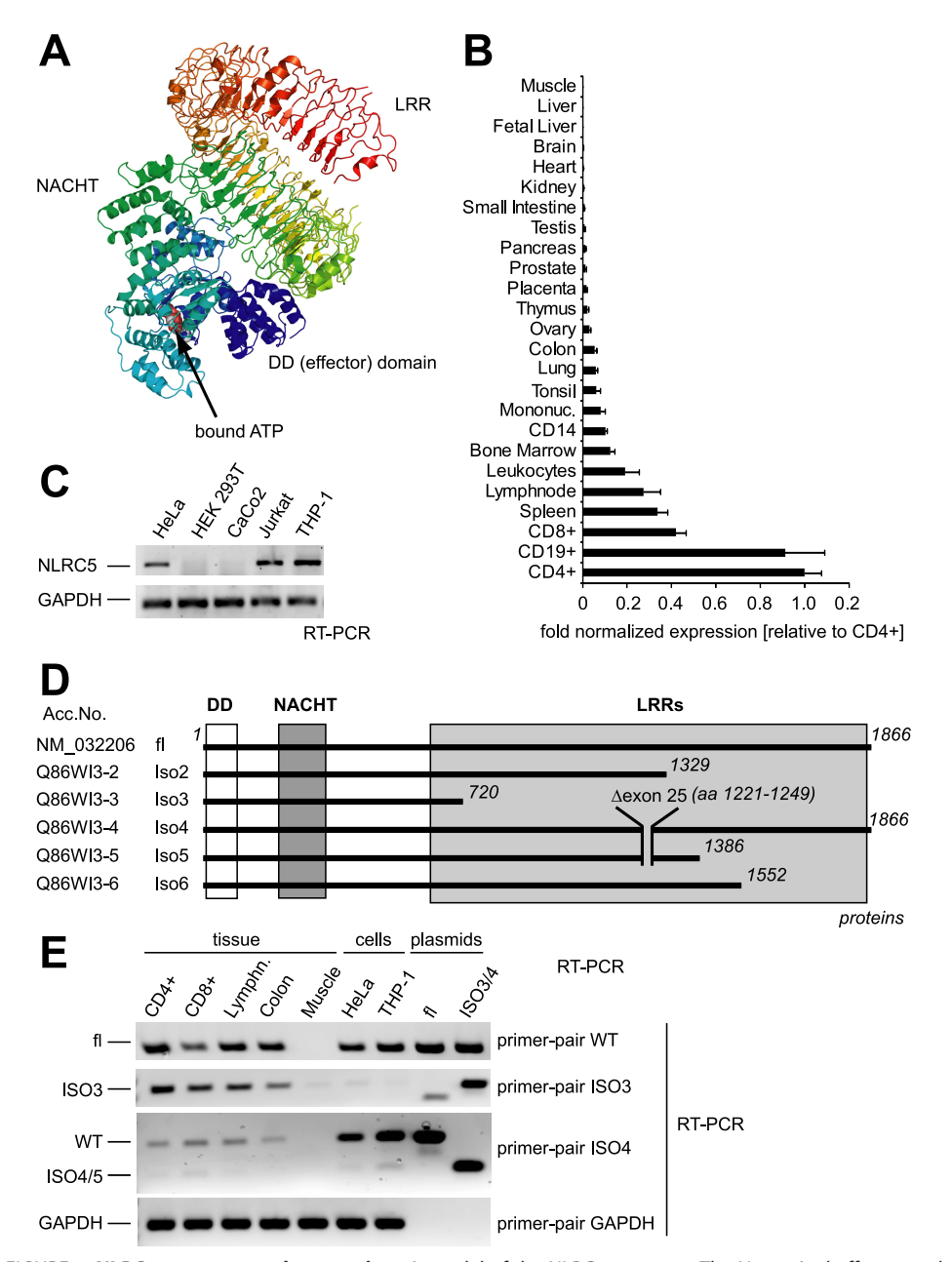


FIGURE 1. **NLRC5 structure and expression.** *A*, model of the NLRC5 structure. The N-terminal effector and NACHT domain with a bound ATP molecule (*blue*) are based on the Apaf-1 effector domain structure (Protein Data Bank entry 126t). The C-terminal LRRs (*red* to *yellow*) are based on the TLR4 LRRs (Protein Data Bank entry 2264). The figure was prepared with Pymol. The positions of the domains are indicated. *B*, quantitative PCR analysis of NLRC5 mRNA expression in the indicated human tissue and blood cells. The expression level of NLRC5 mRNA normalized to GAPDH expression relative to NLRC5 expression in CD4+ cells (set to 1) ± S.D. (*n* = 3) is shown. The order was determined by increasing expression levels. *C*, RT-PCR analysis of NLRC5 mRNA expression in the indicated cell culture lines. Amplification of GAPDH served as control. *D*, schematic representation of putative NLRC5 splice variants. Position of the DD, NACHT, and LRR domains are indicated by *shaded boxes*. The *italic numbers* refer to amino acid (*aa*) positions. *E*, RT-PCR analysis of the indicated tissue and cell culture lines using specific primer pairs to amplify NLRC5 full-length and isoform 3 expression and to detect the deletion in isoform 4 and 5 mRNA. Plasmids encoding NLRC5 full-length (*fl*), isoform 3, or isoform 4 cDNA served as controls. Amplification of GAPDH served as standard. *WT*, wild type.

ities of NLRC5 but might also change the LRR domain from the helical to a classical horseshoe-like structure found in other NLRs. Of note, isoform 3, which lacks the whole LRR region, was the prevalent cDNA obtained during the cloning. This splice variant arises by differential splicing of exon 5 introducing a stop codon in the mRNA. To elucidate the expression of the splice variants ISO3 and ISO4, we con-

structed primer pairs that allowed for the specific amplification of isoform 3 and a primer set able to detect the deletion of exon 25 present in isoform 4 and isoform 5. The selected primer pairs were able to specifically amplify the corresponding isoforms as shown by PCR using plasmids containing the cloned NLRC5 full-length or NLRC5 isoform cDNA (Fig. 1E). According to the presence of ISO3 cDNA in our leukocyte library, we detected NLRC5 isoform 3 in CD4+ and CD8⁺ cells, lymph node, and colon (Fig. 1E). ISO4/5, however, was detected only at low levels in CD4⁺ cells, lymph node, and colon but was more strongly expressed in CD8⁺ cells. In contrast, both isoforms were not detectable in cDNA from muscle where full-length NLRC5 was also not present (Fig. 1E). This also ruled out that the band obtained with the isoformspecific primer pairs was due to DNA contamination. In HeLa and THP-1 cells that express full-length NLRC5, NLRC5 isoform 3 was not robustly detectable; however, isoform 4/5 was expressed at low levels in THP-1 cells (Fig. 1E).

To analyze protein expression of NLRC5, we generated rat monoclonal antibodies specific for NLRC5. The clone 3H8 was able to specifically detect overexpressed NLRC5 from HEK293T cells, migrating at \sim 180 kDa (Fig. 2A). siRNA knockdown experiments in THP-1 cells, using two different siRNAs that had been evaluated by targeting ectopically expressed NLRC5 in HEK293T cells (data not shown), clearly demonstrated the identity of the detected 180-kDa band in THP-1 cells as endogenous NLRC5 (Fig. 2B). NLRC5 has a predicted molecular mass of 204 kDa; the observed somewhat faster migration in SDS-PAGE of both the endogenous and

ectopically expressed protein could be due to the unusually long LRRs, which might adopt a particular compacted structure or harbor post-translational modifications. Of note, we observed a double band for overexpressed NLRC5, whereas endogenous NLRC5 appeared as a single band (Fig. 2, *A* and *B*). This indicated that overexpression might activate NLRC5, leading to post-translational modifications. To explore the subcellular



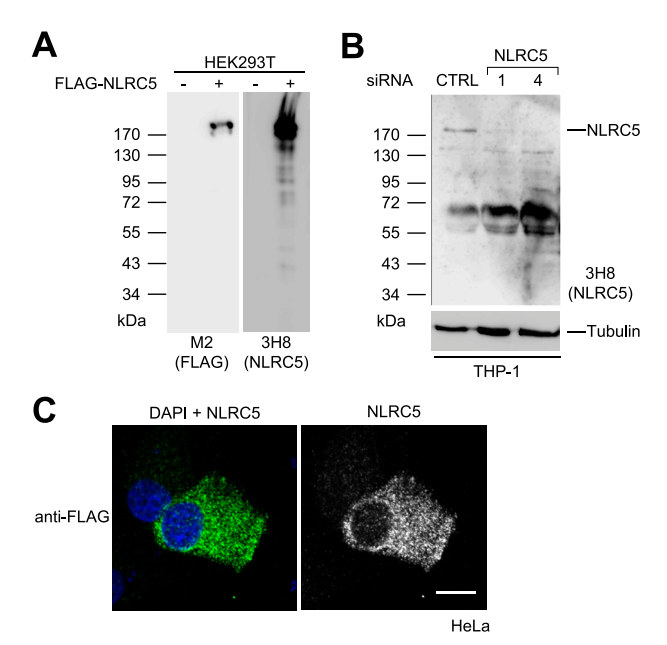


FIGURE 2. **NLRC5 protein expression.** A, characterization of the 3H8 anti-NLRC5 monoclonal antibody. Western blot analysis of lysates of HEK293T (–) and HEK293T cells transfected with FLAG-NLRC5 (+) are shown. As control for expression of the NLRC5 plasmid, a similar blot was probed with anti-FLAG (M2) antibody (left panel). Running of a protein standard is indicated. B, THP-1 cells were treated for 48 h with a control (CTRL) or two NLRC5 specific siRNA duplexes. The cells were lysed in SDS-PAGE loading buffer, and NLRC5 was detected using the 3H8 antibody. Probing for α -tubulin served as a control for equal loading. Running of a protein standard is indicated. C, indirect immunofluorescence micrograph of HeLa cells, transiently transfected with FLAG-NLRC5 using anti-FLAG antibody. Co-staining with 4',6-diamidino-2-phenylindole, dihydrochloride (DAPI, blue) is shown in the left panel. Bar, 10 μ m.

localization, FLAG-NLRC5 was expressed in HeLa cells. This showed that NLRC5 exhibited a cytoplasmic localization (Fig. 2C). Taken together, our data support the presence of multiple splice variants of NLRC5 and demonstrated that NLRC5 is expressed predominantly in tissues of the hematopoietic system in humans, suggesting an involvement of NLRC5 in immune specific pathways.

NLRC5 Induction and Signaling—Expression of many NLRs is induced by PAMPs and inflammatory cytokines. For example, NOD2 expression is up-regulated by bacterial challenge, single-stranded RNA, IFN-γ, and tumor necrosis factor (8, 18, 19). Furthermore, it was recently shown that NF-κB-mediated signaling is a prerequisite of NLRP3 activation by inducing NLRP3 expression (20). We therefore asked whether NLRC5 expression might also be influenced by PAMP stimulation and/or inflammatory mediators. In a first set of experiments THP-1 cells were treated with a variety of bacterial PAMPs and tumor necrosis factor. All of the tested compounds induced inflammatory responses in the cells, monitored by induction of interleukin-8 mRNA. However, no obvious changes in NLRC5 mRNA levels were observed (Fig. 3A). We next used HeLa cells, which, compared with THP-1 cells, showed a lower although detectable basal NLRC5 mRNA expression (Fig. 1C). Treatment with the TLR3 ligand poly(I·C), a double-stranded RNA mimic, robustly increased the mRNA expression of NLRC5 in these cells (Fig. 3B). Moreover, whereas NLRC5 protein levels were at the detection limit in untreated HeLa cells, NLRC5

was robustly detectable after 24 h of poly(I·C) treatment (Fig. 3C). In contrast, poly(I·C) did not significantly induce NLRC5 mRNA (data not shown) or protein levels in THP-1 cells (Fig. 3C). Furthermore, poly(I·C) failed to induce NLRC5 expression in the colon cell line CaCo2 (Fig. 3C). CaCo2 cells are known to be deficient of TLR3 signaling (21, 22), indicating that NLRC5 expression is induced by poly(I·C) in a TLR3-dependent manner. To substantiate that the induction of NLRC5 was mediated by the TLR3 pathway and not by other pattern recognition receptors activated by poly(I·C), siRNA-mediated knockdown of TLR3 and its downstream kinase TBK1 were performed. Efficient knockdown of TBK1 was assured by Western blot analysis (Fig. 3D) and demonstrated that NLRC5 induction by poly(I·C) was mediated by the TLR3/TBK1 pathway (Fig. 3D). In line with the up-regulation by poly(I·C), infection of cells with the single-stranded RNA containing Sendai virus (SeV) led to an approximately 6-fold increase in NLRC5 mRNA levels in HeLa cells (Fig. 3E) and increased protein expression (Fig. 3F). In contrast, as with poly(I·C), only a marginal (below 2-fold) induction of NLRC5 mRNA was obtained in THP-1 cells upon SeV infection (Fig. 3*E*). This showed that not only double-stranded RNA but also single-stranded RNA or other viral signatures on SeV are able to induce NLRC5 expression. Furthermore, these experiments revealed that NLRC5 is differentially inducible in different cell types.

Next, we wanted to elucidate the signaling pathways linked to NLRC5. For the NLR proteins NOD1 and NOD2, it is well documented that overexpression in human cells induces autoactivation, which is mediated by oligomerization of these proteins (23, 24). We assumed that this property is shared by NLRC5. Indeed, overexpression of NLRC5 in HEK293T cells induced specific homo-oligomerization of NLRC5, whereas NLRC5 did not strongly interact with NLRP3 or NOD1 (Fig. 4A). Increasing amounts of NLRC5 were expressed in HEK293T cells, and activation of inflammatory pathways was monitored using luciferase-reporter constructs. NF-κB, IFN-β, IRF3 (data not shown), IRF7, and ISRE reporter were tested, because they represent the most relevant innate immune pathways induced by viral and bacterial pathogens. Whereas appropriate controls significantly induced these reporters in our system, no activation was observed upon NLRC5 overexpression (Fig. 4B). To rule out the possibility that the failure of NLRC5 to induce inflammatory pathways was due to negative regulation by its LRRs, we repeated the experiments with a form of NLRC5 lacking the LRR domain (Isoform 3; Fig. 1D). This protein when overexpressed in HEK293T cells formed a SDS stable dimer, likely being indicative for robust autoactivation (data not shown). However, using this construct we obtained virtually the same result as with full-length NLRC5 (data not shown), suggesting that NLRC5 indeed is unable to activate the tested pathways upon overexpression in HEK293T cells.

In conclusion, NLRC5 overexpression failed to induce the tested canonical inflammatory pathways in HEK293T cells, suggesting either that an essential adaptor for NLRC5 signaling is lacking in HEK293T cells or that NLRC5 is linked to signaling pathways that have not been tested here.



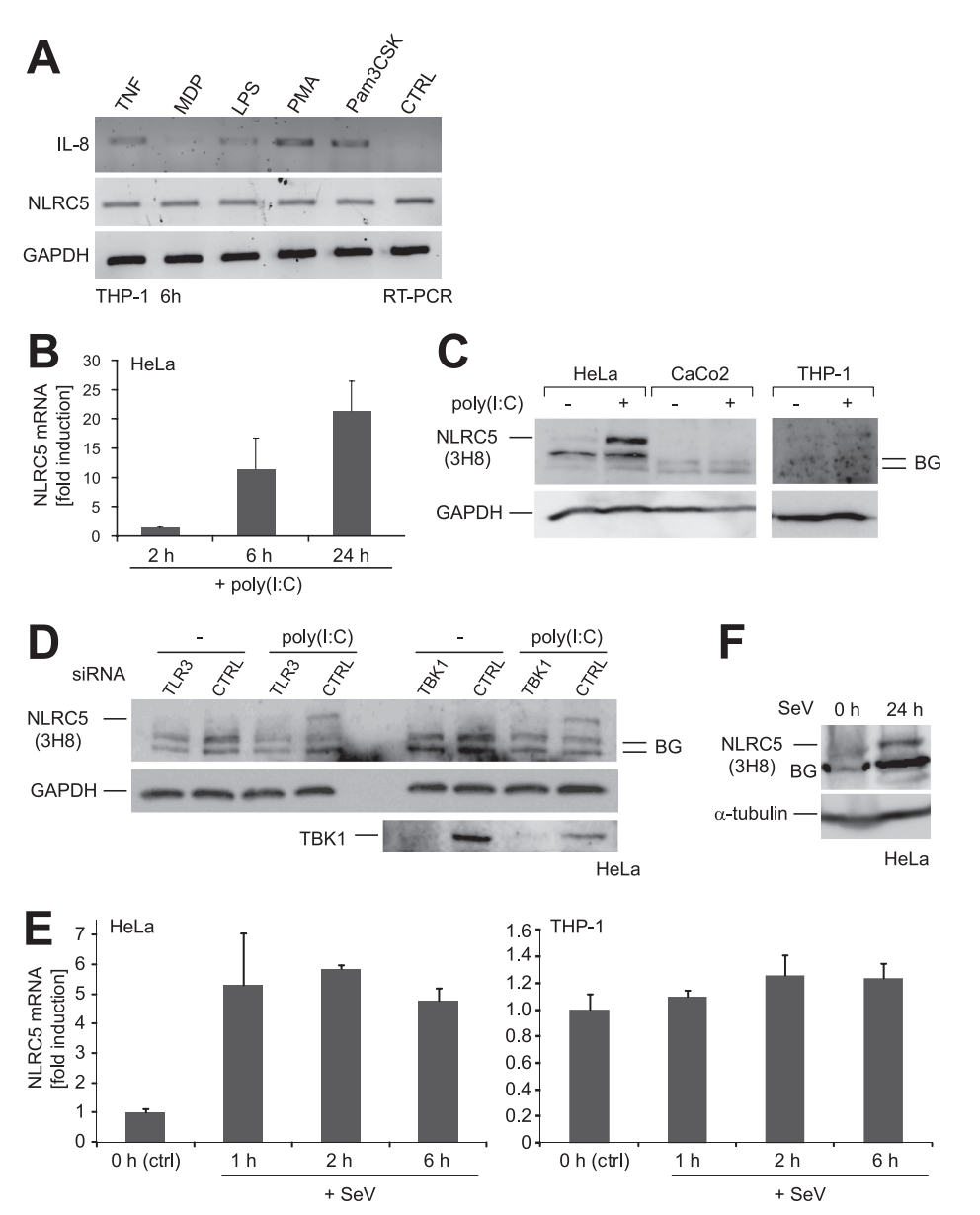


FIGURE 3. Induction of NLRC5 expression by viral PAMPs. A, mRNA levels of NLRC5 after PAMP treatment in THP-1 cells. THP-1 cells were treated with 50 ng/ml tumor necrosis factor (TNF), 1 μM muramyl di-peptide (MDP), 50 ng/ml lipopolysaccharide (LPS), 0.5 μ M phorbol 12-myristate 13-acetate (PMA), or 100 ng/ml Pam3CSK. 6 h after PAMP stimulation, RNA was prepared, and RT-PCRs were conducted amplifying NLRC5 and GAPDH cDNA as control. Interleukin-8 cDNA amplification served as an internal control for successful stimulation. B, quantitative PCR analysis of NLRC5 expression in HeLa cells treated for the indicated time with 100 μ g/ml poly(I-C). The data are normalized to GAPDH expression (n=3). C, Western blot analysis of HeLa, CaCo2, and THP-1 cells treated for 24 h with $100 \mu g/ml$ poly(I-C). Detection with the anti-NLRC5 antibody 3H8 is shown. Probing with a GAPDH-specific antibody served as loading control. BG indicates background bands. D, HeLa cells were treated for 48 h with either TAK1- or TBK1-specific siRNA or nontargeting siRNA (CTRL) as control. The cells were stimulated for an additional 24 h with 100 μ g/ml poly(I·C) where indicated or left untreated (–). Probing with a GAPDH-specific antibody served as loading control. Knockdown of TBK1 is shown by probing with specific antibody (bottom panel). E, quantitative PCR analysis of NLRC5 expression in HeLa and THP-1 cells treated for the indicated time with Sendai virus. The data are normalized to GAPDH expression (n = 3). F, Western analysis of HeLa cells treated for 24 h with Sendai virus. Detection with the anti-NLRC5 antibody 3H8 is shown. Probing for α -tubulin served as a loading control.

NLRC5 Involvement in Mounting Interferon Responses to Viral Infection—Because we observed that Sendai virus and poly(I·C) induced NLRC5 expression, we next wanted to elucidate a possible role for NLRC5 in viral recognition. To explore whether endogenous NLRC5 might have an impact on SeV-mediated responses, we set up a system to conduct siRNA-mediated gene knockdown in phorbol 12-myristate 13-acetate

differentiated THP-1 cells, because they showed the highest basal expression of NLRC5 (Fig. 1C). siRNA transfected cells were treated for 16 h with SeV and supernatant, and cells were collected. Type I interferons are predominately induced by SeV in human cells (25). We therefore measured secreted IFN- α/β using a type I interferon-specific reporter cell line-based bioassay. NLRC5 knockdown reduced secretion of IFN-β compared with mock treatment with a nontargeting siRNA (control) (Fig. 5A). NLRC5 knockdown efficiency was controlled in cell lysates of the same experiment and showed robust reduction of NLRC5 protein levels (Fig. 5B). Moreover, we measured IFN-β mRNA levels by quantitative RT-PCR simultaneously from the same experiments. In correlation with the bioassay data, IFN-β levels were strongly induced by Sendai virus but showed a reduced induction in cells lacking NLRC5 (Fig. 5C). This was also observed for IP-10 (CXCL10) mRNA, another target of the interferon pathway (data not shown). Although the results were highly reproducible, variances in the siRNA efficiency between experiments impaired the generation of highly significant results. Importantly, however, reduction of the cytokine responses correlated with the knockdown efficiency of the two siRNA duplexes used, making it unlikely that the effect was due to off-target effects of the used siRNAs.

To substantiate these results, we also assayed SeV-induced cytokines in THP-1 cells treated with the NLRC5 siRNA in comparison with mock treated cells. This showed a reduced release of RANTES (CCL5), MIP1 α (CCL3), and IP-10, all cytokines well known to be induced by

SeV in primary human cells (25, 26) (supplemental Fig. S1). Significant reduction of RANTES secretion in NLRC5 knockdown cells was confirmed by ELISA (Fig. 5*D*). RT-PCR confirmed reduced RANTES mRNA expression in cells lacking NLRC5 after SeV challenge (Fig. 5*E*). Furthermore, poly(I·C)-induced type I interferon responses were also reduced in THP-1 cells lacking NLRC5 (data not shown).



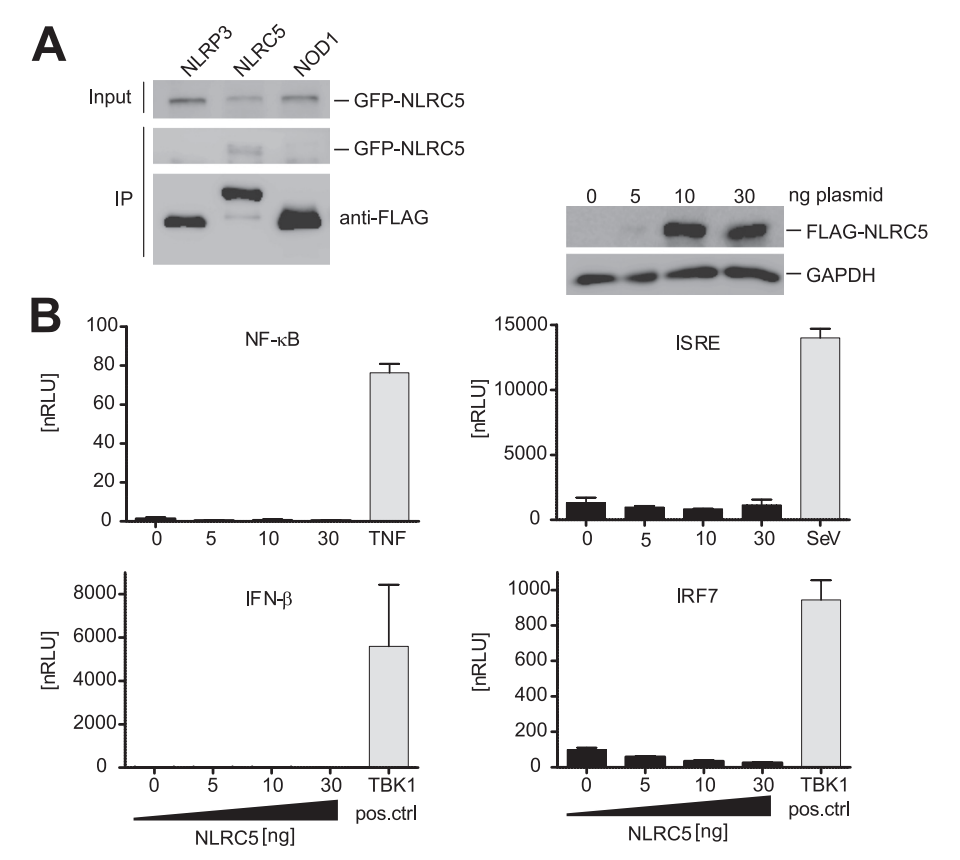


FIGURE 4. NLRC5 signaling. A, co-immunoprecipitation of FLAG-tagged NLR proteins and GFP-NLRC5 transiently expressed in HEK293T cells. FLAG NLRs were precipitated with anti-FLAG antibody, and GFP-NLRC5 was detected in the lysate (Input) and the immunoprecipitations (IP). B, effect of overexpression of NLRC5 on the indicated pathways. HEK293T cells were transfected with increasing amounts (5, 10, and 30 ng) of FLAG-NLRC5 along with the indicated luciferase reporter constructs in 96-well plates. TBK1 overexpression, tumor necrosis factor treatment, or Sendai virus infection served as positive control for the reporter. Read-out was performed 16 h after transfection. Normalized relative light units (nRLU) of triplicate measurements \pm S.D. representative of three independent experiments are shown. Upper right inset, Western blot showing expression of NLRC5 in the ISRE assay. Probing for GAPDH served as a loading control.

To expand our results to primary cells, we used primary human dermal fibroblasts. As observed for HeLa cells, treatment of human fibroblasts with 100 μg/ml poly(I·C) for 16 h led to significant induction of type I interferons (Fig. 6B) and induced NLRC5 mRNA expression in cells derived from two different donors (male and female) (Fig. 6A). Next we conducted siRNA-mediated knockdown of NLRC5 in these cells for 72 h. Knockdown of NLRC5 with two different siRNA duplexes led to reduced type I interferon and RANTES release both after poly(I·C) and after SeV treatment (Fig. 6, B and C). As seen in THP-1 cells both siRNA duplexes reduced the responses to different levels, correlating to their knockdown efficiency as evaluated by RT-PCR from the same experiment (Fig. 6D). These results were further confirmed in cells derived from a third donor, where again a good correlation between knockdown efficiency measured by quantitative PCR and phenotype was obtained (supplemental Fig. S2). Although all donors showed slight variations in the response to poly(I·C) and SeV, the quality of the responses upon NLRC5 knockdown was comparable in all experiments. This led us to conclude that NLRC5 is needed for the efficient induction of anti-viral responses induced by the interferon pathway in human cells.

DISCUSSION

Here we report on the characterization of human NLRC5. Alignment of its LRR and NACHT domains shows that NLRC5 is related to the NLRs NOD1, NOD2, and NLRC3 (5-7), which are involved in the regulation of innate immune responses. NLRC5 is an interesting exception in the NLR family because it (i) contains an effector domain that adopts a DD fold but lacks recognizable homology to the CARD and PYD domains found in other NLRs and (ii) has an unusually long LRR domain. Modeling of this LRR domain of NLRC5 suggested that it forms a large helical conformation (Fig. 1A). However, because this interpretation is purely based on modeling, it is also possible that it adopts a torroid-like structure or connected circles as recently proposed by others (5). The LRR domains of the human NLR proteins are essential for sensing of their cognate PAMPs and DAMPs (2). Furthermore, evidence for changes of the LRR composition of innate immune receptors exists. One intriguing example is given by the ancient VLR proteins in agnathes, which can generate diverse sensing variety by changing the composition of their LRR domains (27). The

unusual structure of the NLRC5 LRR domain might thus be indicative for NLRC5 to respond to quite different stimuli than other NLRs. Accordingly, the isoforms of NLRC5 described here that encoded for changed LRR structures might give rise to changed elicitor sensing spectra of the corresponding proteins. Although the detailed biological function of these NLRC5 isoforms awaits establishment in vivo, we found tissue-specific expression of at least two splice variants of NLRC5 lacking the LRRs or parts thereof. High expression of a variant lacking the whole LRR region (isoform 3) in T cells might be indicative of a regulatory role of the encoded protein in these cells. Future studies shall address in detail the function of this isoform.

NLRC5 mRNA was found to be expressed in hematopoietic cells including monocytes, T cells, and B cells. Of note, this basal expression pattern in primary tissue mimics that of NLRC3, a NLR suggested to be involved in negative regulation of T cells (9), making it tempting to speculate that these two NLRs might be functionally linked. NLRC5 mRNA and protein levels were induced by the TLR3 ligand poly(I·C) and Sendai virus infection in nonhematopoietic cells such as HeLa. Thus, NLRC5 is up-regulated by both single-stranded and doublestranded RNA viruses and/or viral signatures. Notably, in



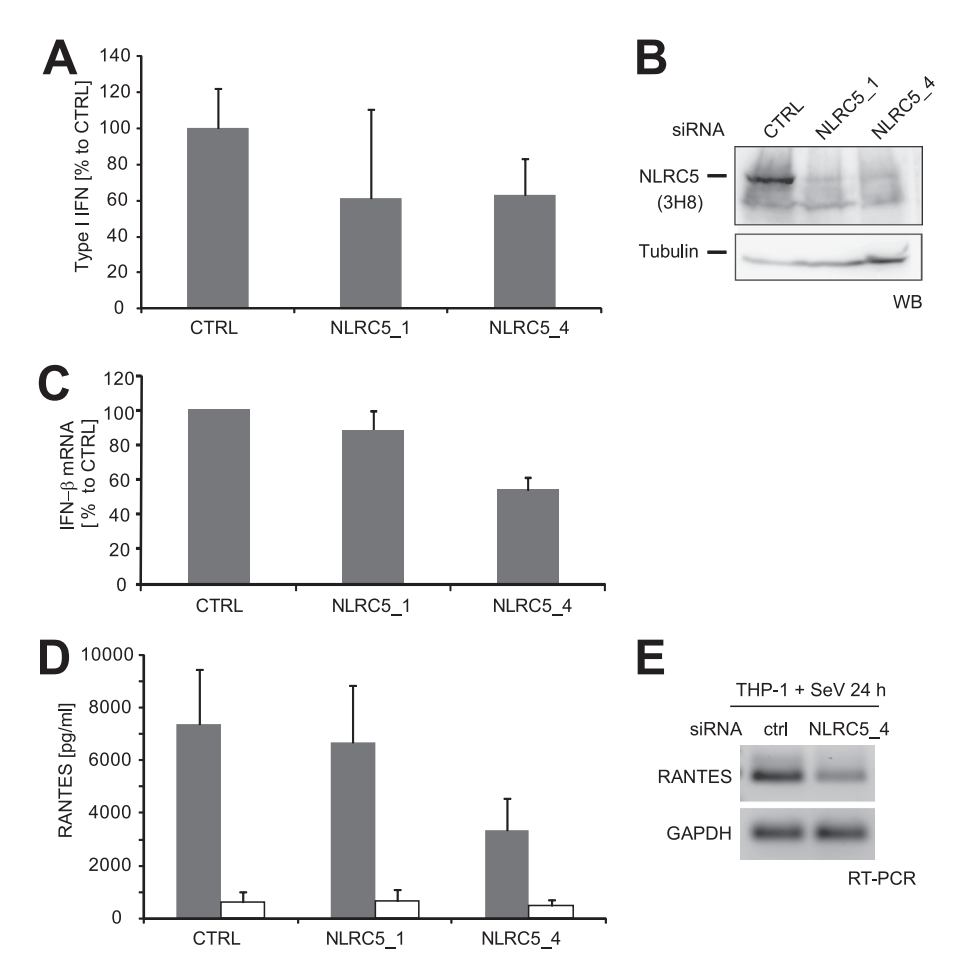


FIGURE 5. **NLRC5 impacts on Sendai virus-mediated type I interferon responses.** THP-1 cells were treated with the indicated siRNA duplexes. 72 h after transfection, the cells were stimulated with Sendai virus or left untreated as controls. A nontargeting siRNA (*CTRL*) was used as negative control. *A*, type I interferon secretion was assayed using a type I interferon secreted alkaline phosphatase reporter cell line (HEK-Blue IFN- α/β)-based bioassay. The data are shown relative to control siRNA set to 100%. *B*, efficient reduction of NLRC5 protein levels shown by Western analysis using the NLRC5-specific 3H8 antibody, probing with α -tubulin served as loading control. *C*, quantitative PCR analysis of IFN- β expression in the cells of *A*. The data are normalized to GAPDH expression (n=2) and are presented relative to CTRL siRNA set to 100%. *D*, RANTES cytokine levels were measured in the supernatant of cells treated as in *A* after 16 h of SeV exposure (*gray bars*) or mock treatment (*white bars*). *E*, RT-PCR analysis of RANTES mRNA expression in THP-1 cells treated with control (*ctrl*) or NLRC5_4 siRNA for 72 h prior to SeV exposure for 24 h. Amplification of GAPDH served as a loading control.

THP-1 cells we only observed a marginal induction of NLRC5 levels after poly(I·C) and Sendai virus challenge, respectively (Fig. 3). In line with the observed high basal NLRC5 expression in THP-1 cells and its low expression in HeLa cells, this suggests that NLRC5 expression is differentially regulated in various cell types; although myeloid cells have already high basal expression levels of NLRC5, assuring sufficient response to the cognate stimulus, nonhematopoietic cells might be required to gain NLRC5 competence by induction of NLRC5 expression upon exposure to inflammatory milieu. Such a positive feedback loop is known for other NLRs. Although our data, in particular direct targeting of the TLR3 pathway, suggested that NLRC5 expression is under direct control of the type I interferon pathway, we cannot exclude that the induction is due to release of secondary effectors upon interferon activation by an autocrine loop.

To elucidate the molecular connection of NLRC5 to innate immune pathways, we further aimed to identify interaction

partners and signaling pathways linked to the NLRC5 effector domain. Kuenzel et al. (28) recently reported activation of a ISRE and GAS reporter induced by overexpression of a GFP-tagged version of NLRC5 and forced dimerization of the NLRC5 death domain in HeLaS3 cells. We, however, could not observe activation of an ISRE reporter also with an N-terminal GFP-tagged version of NLRC5 in HEK293T (data not shown), suggesting that HEK293T cells might lack an essential adaptor for NLRC5 signaling. In line, overexpression of NLRC5 did not yield activation of other canonical inflammatory pathways in HEK293T cells (Fig. 4), including p38 MAPK (data not shown). We thereby can exclude that a putative negative regulation by the LRR domain as a form of NLRC5 lacking the LRR domain (isoform 3) led to the same results. In contrast, overexpression of NLRC5 significantly impaired type I interferon reporter activation in HEK293T cells without affecting NF-kB responses, supporting a role for NLRC5 in type I interferon responses (supplemental Fig. S3). This effect was likely due to titration of a factor involved in the type I interferon pathway. Co-immunoprecipitation experiments using educated guesses, including TBK1, SINTBAD, TANK1, NAP1, IKK ϵ , and IRF3, 7, and 5, as well as unbiased yeast two-hybrid screening of

NLRC5 and its DD, were conducted to address this observation in more detail (data not shown). Unfortunately, the results did not allow us to link NLRC5 to any known component of the type I interferon pathway yet. Of note, recent studies also failed to reveal robust interactions between NLRC5 and known NLR adaptor proteins such as RIP2K and ASC (29, 30).

However, clear physiological evidence for a role of NLRC5 in anti-viral responses could be obtained by controlled siRNA studies in the myeloid-like THP-1 cell line. Knockdown of endogenous NLRC5 in these cells robustly impaired the type I interferon response as shown by reduced IFN- β release and lower IFN- β and IP-10 mRNA induction upon SeV infection (Fig. 5 and supplemental Fig. S1). We expanded these findings by analyzing other SeV-induced cytokines (supplemental Fig. S1). This revealed that among others the induction and release of the important early phase chemokine RANTES (CCL5) was also negatively affected upon NLRC5 knockdown (Fig. 5). RANTES is known to be released upon SeV infection also from primary



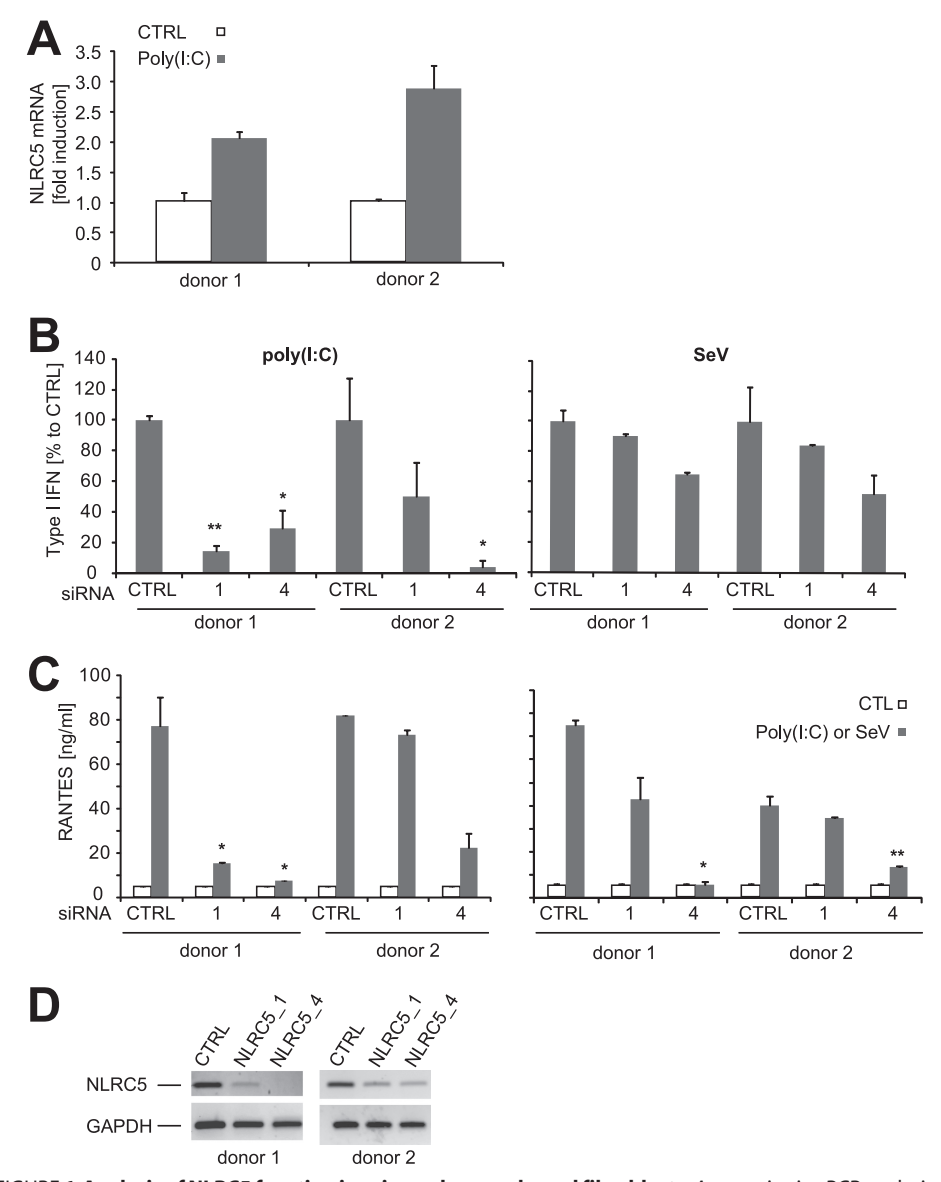


FIGURE 6. Analysis of NLRC5 function in primary human dermal fibroblasts. A, quantitative PCR analysis of NLRC5 expression in cells treated for 24 h with 100 μ g/ml poly(I-C). The data are normalized to GAPDH expression. CTRL, mock treated cells. B, cells were treated with the indicated NLRC5-specific siRNA duplexes (columns 1 and 4) for 72 h and subsequently stimulated with poly(I-C) (left panel) or Sendai virus (right panel). A nontargeting siRNA (CTRL) was used as a negative control. Type I interferon secretion was assayed using a type I interferon secreted alkaline phosphatase reporter cell line (HEK-Blue IFN- α/β)-based bioassay. The data are shown relative to CTRL siRNA set to 100%. C, RANTES cytokine levels measured in the supernatant of cells of B after 16 h of induction with poly(I·C) or SeV (gray bars) or mock treatment (white bars). D, RT-PCR analysis of NLRC5 mRNA expression in the cells shown in B and C treated with control (CTL) or NLRC5 siRNA for 72 h. Amplification of GAPDH served as a loading control.

human cells (25, 26). Indeed, we could substantiate the observation made in THP-1 cells in primary human dermal fibroblast from different donors (Fig. 6) where knockdown of NLRC5 by two different siRNA duplexes led again to a robust reduction of both SeV- and poly(I·C)-induced type I interferon and RANTES release in these cells. Importantly, IP-10, IFN- β , and RANTES induction is directly dependent on activation of IRF3 by the interferon pathway (31, 32), suggesting that NLRC5 has an impact on this pathway. In conclusion, our data show that NLRC5 is involved in regulating the type I interferon pathway.

Taken together, our data support a role for NLRC5 in viral innate immune responses and put it on the list of NLR proteins with proposed functions in viral recognition such as NLRP3 (33-35), NOD2 (8, 36), and NLRX1 (37). Of note, all of these NLRs respond to RNA signatures.

We furthermore attempted to decipher the cognate PAMP(s) for NLRC5 by testing known PAMPs. However, lipopolysaccharide, single-stranded RNA, E. coli RNA, poly(I·C), as well as TLR5 and TLR6 ligands failed to activate robust NLRC5-mediated interferon or NF-κB responses in HEK293T cells (data not shown).

Because the molecular function of NLRC5 still remains somewhat elusive, we currently can only speculate on its precise mode of function. One tempting assumption is that NLRC5 might act in conjunction with other NLRs. Evidence for the existence of such NLR networks exists (38). Furthermore, NOD2 and NLRP10 have been recently identified as factors involved in mounting interferon responses toward influenza virus infection (36), and NOD2 might even be able to directly detect single-stranded RNA (8). It therefore is noteworthy that we observed a physical interaction of NLRC5 with both NOD2 and NLRP10 in a NACHT-dependent manner using overexpressed proteins.3 Although the biological relevance of these findings remains elusive for endogenous proteins, one could envision a scenario where NLRC5 might not only induce responses to viral infections but at the same time might impact on NOD2-mediated responses.

Further studies are needed to understand the function of this interesting new NLR protein in innate immune responses to viral pathogens

and its interplay with other NLR members in more detail. Based on our results, however, we assume that a lack of NLRC5 or hypomorphs negatively affects the fitness of the host upon viral

During the preparation of this manuscript, NLRC5 was found independently to have a role also in cytomegalovirus-induced immune responses (28). This further supports our findings and suggests that NLRC5 might be involved in anti-viral responses

³ A. Neerincx, K. Lautz, M. Menning, R. Schwarzenbacher, and T. A. Kufer, unpublished results.



more in general because cytomegalovirus contains a double-stranded DNA genome.

Acknowledgments—We thank Birte Zurek and Harald Bielig for helpful discussions, Jörg Fritz (University of Toronto) for critical comments on the manuscript, and Martin Krönke (University of Cologne) for continuous support.

REFERENCES

- 1. Akira, S., Uematsu, S., and Takeuchi, O. (2006) Cell 124, 783-801
- Fritz, J. H., Ferrero, R. L., Philpott, D. J., and Girardin, S. E. (2006) Nat. Immunol. 7, 1250 –1257
- 3. Kufer, T. A. (2008) Mol. Biosyst. 4, 380 386
- 4. Martinon, F., Mayor, A., and Tschopp, J. (2009) Annu. Rev. Immunol. 27, 229–265
- 5. Istomin, A. Y., and Godzik, A. (2009) BMC Immunol. 10, 48
- 6. Hughes, A. L. (2006) Immunogenetics 58, 785-791
- Proell, M., Riedl, S. J., Fritz, J. H., Rojas, A. M., and Schwarzenbacher, R. (2008) PLoS One 3, e2119
- Sabbah, A., Chang, T. H., Harnack, R., Frohlich, V., Tominaga, K., Dube, P. H., Xiang, Y., and Bose, S. (2009) *Nat. Immunol.* 10, 1073–1080
- Conti, B. J., Davis, B. K., Zhang, J., O'connor, W., Jr., Williams, K. L., and Ting, J. P. (2005) J. Biol. Chem. 280, 18375–18385
- 10. Ting, J. P., and Davis, B. K. (2005) Annu. Rev. Immunol. 23, 387–414
- 11. Zigrino, P., Drescher, C., and Mauch, C. (2001) Eur. J. Cell Biol. 80, 68-77
- Kufer, T. A., Kremmer, E., Adam, A. C., Philpott, D. J., and Sansonetti, P. J. (2008) Cell Microbiol. 10, 477–486
- Matsukura, S., Kokubu, F., Kubo, H., Tomita, T., Tokunaga, H., Kadokura, M., Yamamoto, T., Kuroiwa, Y., Ohno, T., Suzaki, H., and Adachi, M. (1998) Am. J. Respir. Cell Mol. Biol. 18, 255–264
- Quasdorff, M., Hösel, M., Odenthal, M., Zedler, U., Bohne, F., Gripon, P., Dienes, H. P., Drebber, U., Stippel, D., Goeser, T., and Protzer, U. (2008) Cell Microbiol. 10, 1478 –1490
- Li, K., Chen, Z., Kato, N., Gale, M., Jr., and Lemon, S. M. (2005) J. Biol. Chem. 280, 16739 – 16747
- Sharma, S., tenOever, B. R., Grandvaux, N., Zhou, G. P., Lin, R., and Hiscott, J. (2003) Science 300, 1148–1151
- Bielig, H., Zurek, B., Kutsch, A., Menning, M., Philpott, D. J., Sansonetti,
 P. J., and Kufer, T. A. (2009) *Mol. Immunol.* 46, 2647–2654
- Oh, H. M., Lee, H. J., Seo, G. S., Choi, E. Y., Kweon, S. H., Chun, C. H., Han,
 W. C., Lee, K. M., Lee, M. S., Choi, S. C., and Jun, C. D. (2005) Cell. Immunol. 237, 37–44
- Rosenstiel, P., Fantini, M., Bräutigam, K., Kühbacher, T., Waetzig, G. H., Seegert, D., and Schreiber, S. (2003) Gastroenterology 124, 1001–1009

- Bauernfeind, F. G., Horvath, G., Stutz, A., Alnemri, E. S., MacDonald, K., Speert, D., Fernandes-Alnemri, T., Wu, J., Monks, B. G., Fitzgerald, K. A., Hornung, V., and Latz, E. (2009) J. Immunol. 183, 787–791
- Alexopoulou, L., Holt, A. C., Medzhitov, R., and Flavell, R. A. (2001) Nature 413, 732–738
- Vijay-Kumar, M., Gentsch, J. R., Kaiser, W. J., Borregaard, N., Offermann, M. K., Neish, A. S., and Gewirtz, A. T. (2005) *J. Immunol.* 174, 6322–6331
- Inohara, N., Koseki, T., Lin, J., del Peso, L., Lucas, P. C., Chen, F. F., Ogura, Y., and Núñez, G. (2000) J. Biol. Chem. 275, 27823–27831
- Ogura, Y., Inohara, N., Benito, A., Chen, F. F., Yamaoka, S., and Nunez, G. (2001) J. Biol. Chem. 276, 4812–4818
- Hua, J., Liao, M. J., and Rashidbaigi, A. (1996) J. Leukocyte Biol. 60, 125–128
- 26. Matikainen, S., Pirhonen, J., Miettinen, M., Lehtonen, A., Govenius-Vintola, C., Sareneva, T., and Julkunen, I. (2000) *Virology* **276**, 138–147
- Pancer, Z., Amemiya, C. T., Ehrhardt, G. R., Ceitlin, J., Gartland, G. L., and Cooper, M. D. (2004) *Nature* 430, 174–180
- Kuenzel, S., Till, A., Winkler, M., Häsler, R., Lipinski, S., Jung, S., Grötzinger, J., Fickenscher, H., Schreiber, S., and Rosenstiel, P. (2010) J. Immunol. 184, 1990 – 2000
- Dowds, T. A., Masumoto, J., Chen, F. F., Ogura, Y., Inohara, N., and Núñez, G. (2003) Biochem. Biophys. Res. Commun. 302, 575–580
- Wagner, R. N., Proell, M., Kufer, T. A., and Schwarzenbacher, R. (2009) *PLoS One* 4, e4931
- Andersen, J., VanScoy, S., Cheng, T. F., Gomez, D., and Reich, N. C. (2008) Genes Immun. 9, 168–175
- Lin, R., Heylbroeck, C., Genin, P., Pitha, P. M., and Hiscott, J. (1999) Mol. Cell. Biol. 19, 959 – 966
- Delaloye, J., Roger, T., Steiner-Tardivel, Q. G., Le Roy, D., Knaup Reymond, M., Akira, S., Petrilli, V., Gomez, C. E., Perdiguero, B., Tschopp, J., Pantaleo, G., Esteban, M., and Calandra, T. (2009) *PLoS Pathog.* 5, e1000480
- Kanneganti, T. D., Body-Malapel, M., Amer, A., Park, J. H., Whitfield, J., Franchi, L., Taraporewala, Z. F., Miller, D., Patton, J. T., Inohara, N., and Núñez, G. (2006) J. Biol. Chem. 281, 36560 –36568
- 35. Muruve, D. A., Pétrilli, V., Zaiss, A. K., White, L. R., Clark, S. A., Ross, P. J., Parks, R. J., and Tschopp, J. (2008) *Nature* **452**, 103–107
- Shapira, S. D., Gat-Viks, I., Shum, B. O., Dricot, A., de Grace, M. M., Wu,
 L., Gupta, P. B., Hao, T., Silver, S. J., Root, D. E., Hill, D. E., Regev, A., and
 Hacohen, N. (2009) Cell 139, 1255–1267
- 37. Moore, C. B., Bergstralh, D. T., Duncan, J. A., Lei, Y., Morrison, T. E., Zimmermann, A. G., Accavitti-Loper, M. A., Madden, V. J., Sun, L., Ye, Z., Lich, J. D., Heise, M. T., Chen, Z., and Ting, J. P. (2008) *Nature* 451, 573–577
- Damiano, J. S., Oliveira, V., Welsh, K., and Reed, J. C. (2004) Biochem. J. 381, 213–219



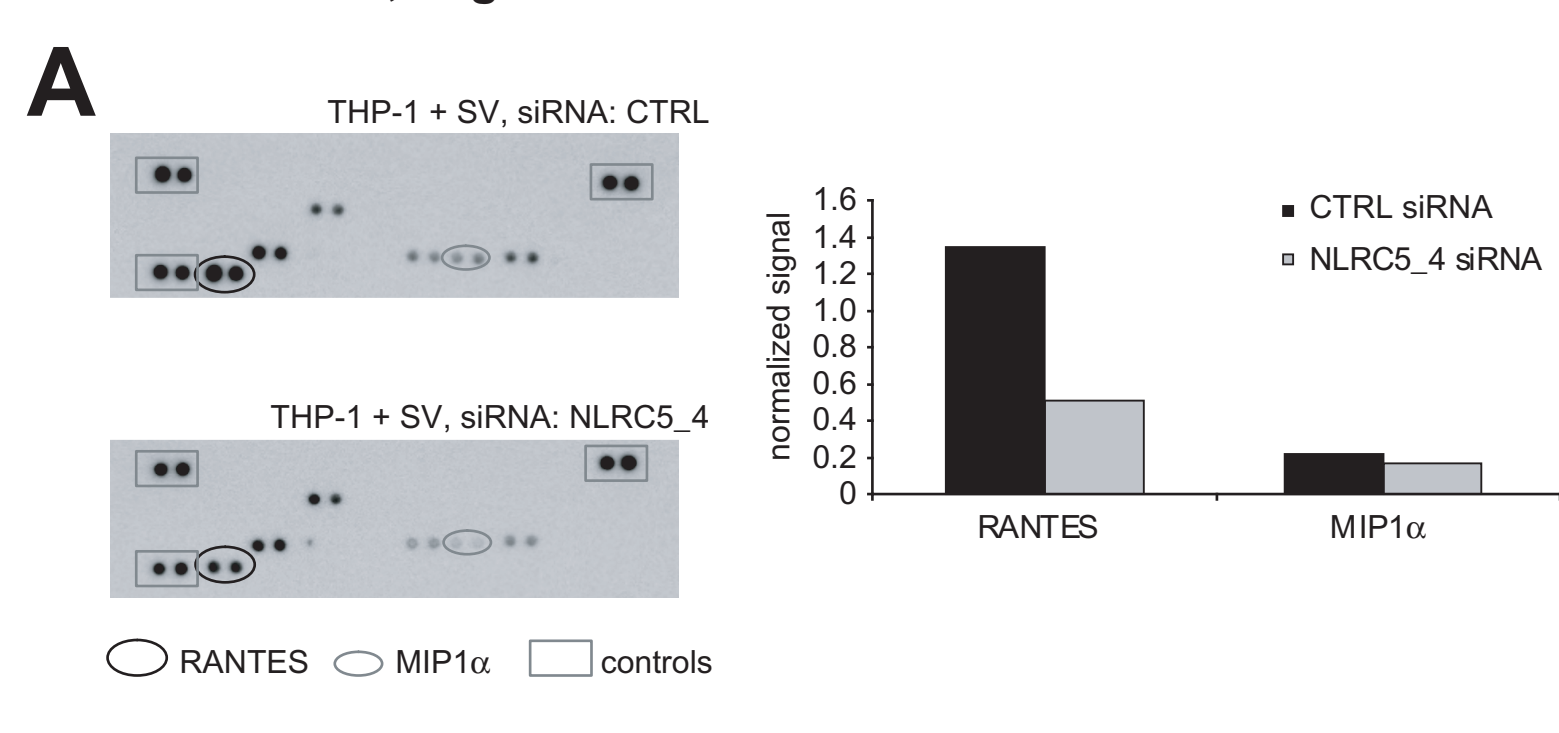
Neerincx et al. supplemental figure legends

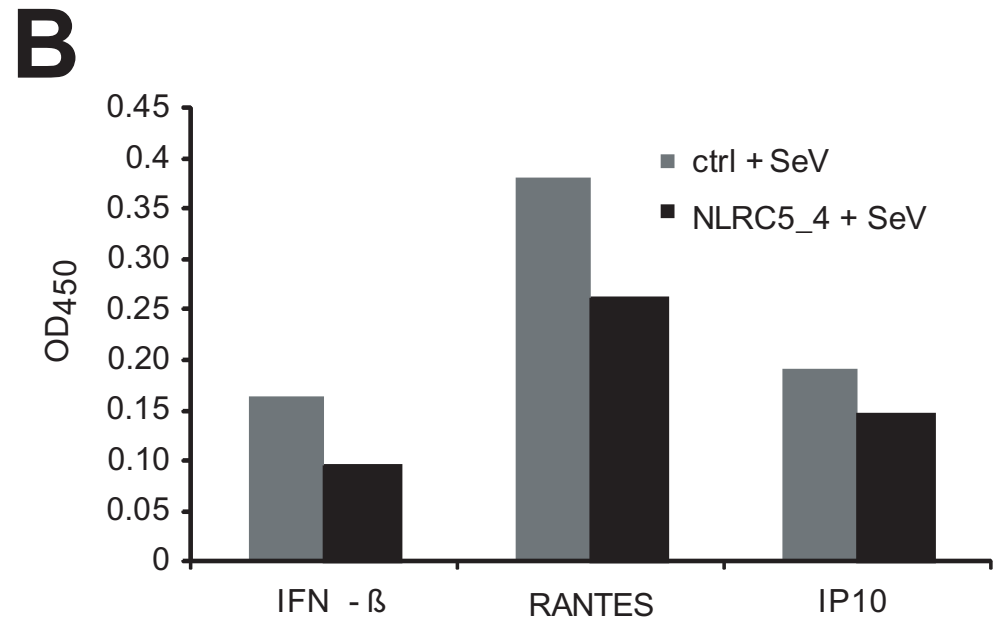
<u>Fig.S1.</u> NLRC5 reduces Sendai virus induced cytokine responses. *A.* Analysis of the cytokine secretion profile after SeV infection of THP-1 cells treated with control siRNA (CTRL) or the NLRC5 specific NLRC5_4 siRNA using a Western-based array. Densitometric quantification of the signals for RANTES and MIP1 α , normalized to the controls are shown in the right panel. *B.* ELISA of the supernatants from (Fig. 5A) for IFN- β , RANTES and IP-10 protein levels.

Fig.S2. Analysis of NLRC5 function in primary human dermal fibroblasts. A. Cells from donor 3 were treated with the indicated NLRC5 specific siRNA duplexes (1 and 4) for 72 h and subsequently stimulated with poly(I:C) (left panel) or SeV (right panel). A non-targeting siRNA (CTRL) was used as negative control. Type I interferon secretion was assayed using a type I interferon SEAP reporter cell-line (HEK-Blue IFNα/β) based bioassay. Data is shown relative to CTRL siRNA set to 100 %. B. RANTES cytokine levels measured in the supernatant of cells of (A) after 16 h of induction with poly(I:C) or SeV (gray bars) or mock treatment (white bars). C. Quantitative PCR analysis of NLRC5 mRNA expression in the cells of (A,B) treated with control (CTL) or NLRC5 siRNAs for 72 h. Expression normalized to GAPDH is shown. n.d.: not detectable.

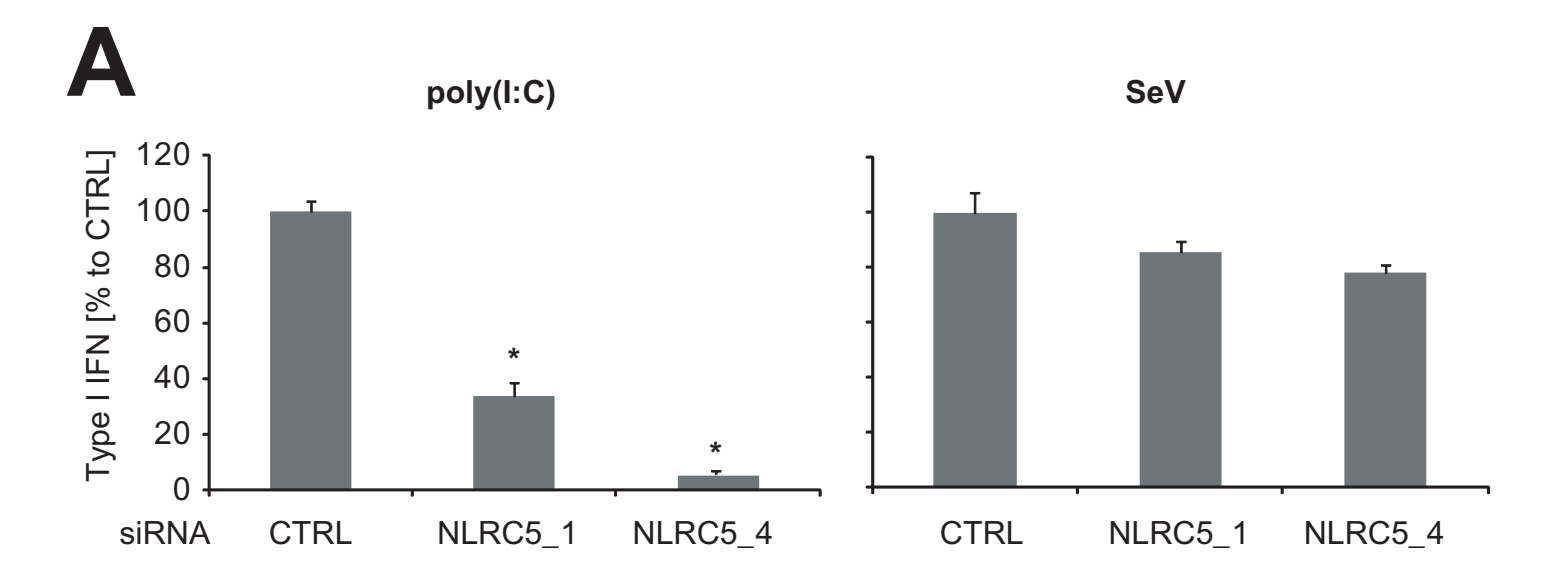
Fig.S3. NLRC5 over-expression negatively influences type I interferon reporter activation in HEK293T cells. A. Effect of NLRC5 on signalling responses in HEK293T cells. The indicated amounts of FLAG-NLRC5 were co-transfected along with a NF-κB responsive reporter plasmid in 96-well plates and cells were treated with 100 ng/ml TNF (upper panel). Alternatively, an IFN-β luciferase reporter construct was transfected and activated by TBK1 over-expression (middle panel) or Sendai virus (lower panel), respectively. Normalized relative light units (RLU) of triplicate measurements, + S.D., representative of three independent experiments are shown.

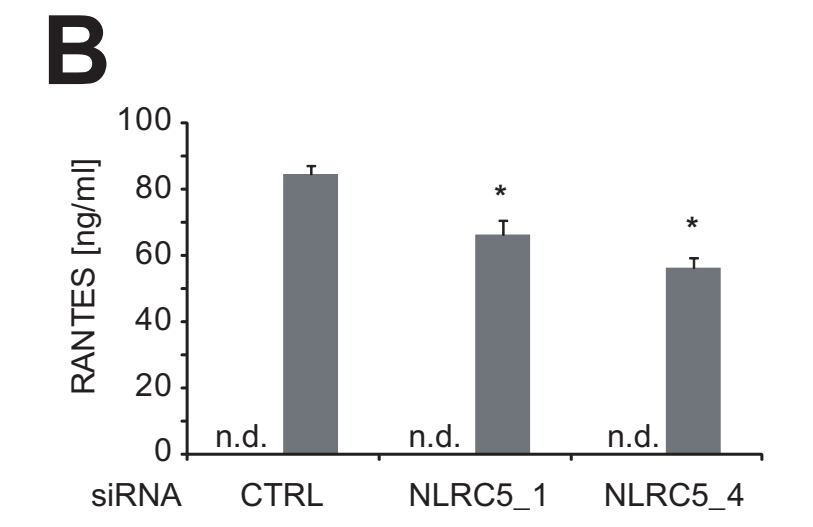
Neerincx et al., Figure S1:

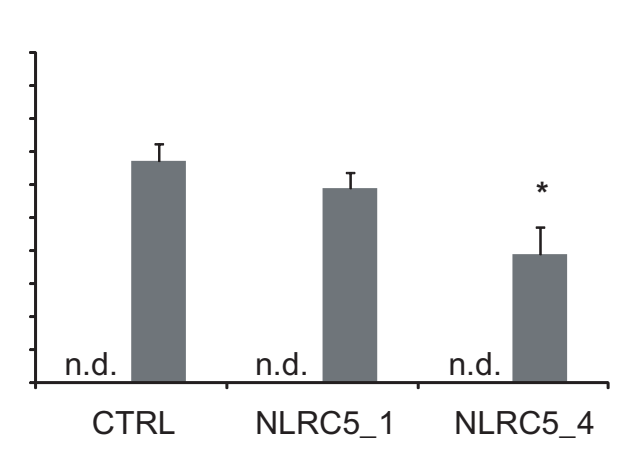


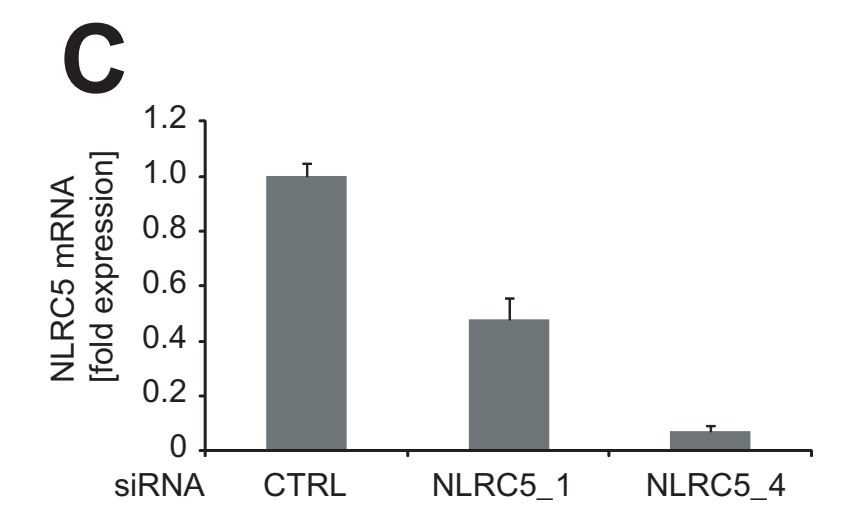


Neerincx et al., Figure S2:









Neerincx et al., Figure S3:

